J|A|C|S
ARTICLES
Published on Web 02/27/2002

Structural Analysis of the Solid Amorphous Binuclear Complexes of Iron(III) and Aluminum(III) with Chromium(III)−DTPA Chelator Using Energy Dispersive X-ray Diffraction

Claudia Sadun,* Remo Bucci, and Antonio L. Magrì

Contribution from the Dipartimento di Chimica, INFM Istituto Nazionale di Fisica della Materia, Università degli Studi di Roma "La Sapienza", P.le A. Moro 5, 00185 Roma, Italy

Received March 13, 2001

Abstract: This paper is concerned with the structural data obtained for two amorphous binuclear complexes of iron(III) and aluminum(III) with chromium(III)−diethylentriaminepentaacetic acid (chromium(III)−DTPA, CrL^{2-}) using the energy-dispersive X-ray diffraction technique. $Fe(OH)CrL(H_2O)_6$ and $Al(OH)CrL(H_2O)_6$ are binuclear complexes, the metals ions being bridged via oxygen atoms. The metal ions are all octahedrally coordinated.

1. Introduction

Major research effort has been devoted to studying complexation reactions of metal ions with inorganic and/or organic ligands. The chemical, physical, biological, and toxicological properties of the new compounds differ from those of the separate constituents.

Magnetic resonance imaging (MRI) for noninvasive investigations of the human body, which require the use of paramagnetic, but nontoxic, contrast media, is one striking example of the progress achieved in this area. There are many metal ions with unpaired spins that are toxic in their native form. Research has focused on creating thermodynamically stable and kinetically inert complexes that, without altering the paramagnetic properties of the metal ion, are much less toxic than both the metal ion and the ligand in the unbound state. Of the compounds tested, certain complexes of strongly paramagnetic metal ions [gadolinium(III), iron(III), and chromium(III)] with diethylenetriaminepentaacetic acid ($C_{14}N_3O_{10}H_{23}$, DTPA, H_5L) would appear to exhibit suitable properties.

Prompted by our research interests in the reaction, structure, and thermodynamics of metal complexes, we turned our attention to the chromium(III)−DTPA (CrL^{2-}) species for the purpose of assessing its complexing ability. This compound is a highly stable and inert species with a noncoordinated iminodiacetate group,[1] and thus it may be used as a new chelator, whose properties will also depend on its "free" or "metal-complex" form.

In earlier papers[2−4] we described the main results of investigations concerning the complexation reaction of this ligand with some divalent metal ions. More recently, we extended the research to the chromium(III)−DTPA reaction with trivalent metal ions (iron(III)[5] and aluminum(III)[6]). In these two cases, a similar 1:1 (metal to ligand molar ratio) complex was found. The weaker acidity of the aqueous solution utilized for the aluminum system also indicated the formation of a mixed complex with hydroxide ion and a 1:2 species. Comparison of the stability constants with those of the corresponding iron(III) and aluminum(III) complexes with iminodiacetic acid suggested that these metal ions are always coordinated by iminodiacetate groups. The IR spectra of the 1:1 solid-state compounds ([$Fe(OH)CrL(H_2O)_6$] and [$Al(OH)CrL(H_2O)_6$]) substantiated this hypothesis though the compounds showed different thermal stability, especially in oxygen atmosphere.

To fully understand the physical and chemical behavior of these complexes, their structure needs to be accurately determined. Wide-angle X-ray scattering (WAXS) has been used as it provides an insight into how metal ions interact with their surroundings.[7] Here the coordination structures of the metal ions in the above complexes have been determined.

The coordination geometry of several metal ions, in amorphous phase, has been studied using the WAXS technique.[8−10] The structures of metal ions−iminodiacetate ligand complexes, in solid crystal state, have been studied elsewhere.[11−13] The

* To whom correspondence should be addressed. E-mail: c.sadun@caspur.it.

(1) Bucci, R.; Magrì, A. L.; Napoli, A. *J. Coord. Chem.* **1991**, *24*, 169.
(2) Napoli, A.; Bucci, R.; Magrì, A. D.; Magrì, A. L. *Ann. Chim. (Rome)* **1991**, *81*, 693.
(3) Belcastro, M.; Napoli, A. *Ann. Chim. (Rome)* **1993**, *83*, 451.
(4) (a) Bucci, R.; Magrì, A. D.; Magrì, A. L.; Napoli, A. *Thermochim. Acta* **1993**, *217*, 213. (b) Bucci, R.; Magrì, A. D.; Magrì, A. L.; Napoli, A. *J. Therm. Anal.* **1996**, *46*, 1865. (c) Bucci, R.; Magrì, A. D.; Magrì, A. L.; Napoli, A. *Ann. Chim. (Rome)* **1998**, *88*, 25.
(5) Bucci, R.; Magrì, A. D.; Magrì, A. L.; Napoli, A. *Polyhedron* **2000**, *19*, 2421.
(6) Bucci, R.; Magrì, A. D.; Magrì, A. L.; Napoli, A. *Anal. Lett.* **2001**, *34*, 6.
(7) Atzei, D.; Ferri, T.; Sadun, C.; Sangiorgio, P.; Caminiti, R. *J. Am. Chem. Soc.* **2001**, *123*, 2552−2558.
(8) Atzei, D.; De Filippo, D.; Rossi, A.; Caminiti, R.; Sadun, C. *Spectrochim. Acta* **1995**, *51A*, 11.
(9) Atzei, D.; De Filippo, D.; Rossi, A.; Caminiti, R.; Sadun, C. *Inorg. Chim. Acta* **1996**, *248*, 203.
(10) Atzei, D.; Sadun, C.; Pandolfi, L. *Spectrochim. Acta* **2000**, *56A*, 531−540.
(11) Caminiti, R.; Cucca, P.; Monduzzi, M.; Saba, G.; Crisponi, G. *J. Chem. Phys.* **1984**, *81*, 543−551.

10.1021/ja010676+ CCC: $22.00

iminodiacetate ion behaves like a tridentate ligand, chelating metal ions via two carboxylate oxygen atoms and the amine nitrogen atom. The metal ion is bound to one or two ligands in an octahedral arrangement via meridional or facial coordination. There is a moderate preference for facial coordination, though a few instances of meridional coordination have been reported. When two iminodiacetate molecules are coordinated to the metal, fac-trans (N,N) or fac-trans (N,O) is obtained.

2. Experimental Section

2.1. Reagents. Diethylenetriaminepentaacetic acid chromium(III) disodium salt hexahydrate (Aldrich), iron(III) perchlorate hydrate (Aldrich), and aluminum(III) perchlorate (Rudi Pont) were used.

Other chemicals were of analytical grade. Distilled−deionized water was used throughout.

2.2. Preparation of the Solid Compound. The iron(III)−chromium(III)−DTPA complex was prepared by adding 25 cm^3 of ethanol to 50 cm^3 of an equimolar (40 mmol dm^{-3}) aqueous solution of iron(III) ions and CrL^{2-} "metal-ligand chelator". The precipitate was filtered off, washed first with a 1:1 water−ethanol mixture and then with ethanol, and finally was vacuum-dried over silica gel. The chemical and thermogravimetric analyses of this compound suggested the formula $FeCrL(OH)(H_2O)_6$.[7]

The aluminum(III)−chromium(III)−DTPA complex was prepared by mixing an equimolar (40 mmol dm^{-3}) aqueous solution of aluminum(III) ions and CrL^{2-} "metal-ligand chelator". The precipitate was filtered off, washed with water, and vacuum-dried over silica gel. The chemical and thermogravimetric analyses of this compound suggested the formula $AlCrL(OH)(H_2O)_6$.[8]

2.3. X-ray Scattering Measurements and Data Processing. The samples were finely pulverized and compressed into pellets. Data were acquired with a custom-built energy-dispersive X-ray diffractometer.[14,15] This device consists of a Seifert X-ray HV generator supplying a water-cooled tungsten X-ray source, with 3.0 kW maximum power. The *bremsstrahlung* component of the X-ray source was used. Operating conditions were as follows: 50 kV high voltage supply; 35 mA current intensity; 1750 W total power; 15.0−45.0 kV energy range.

For acquiring the diffraction spectra, a Germanium solid-state detector (SSD) connected via an electronic chain to a multichannel analyzer was used. The diffractometer is completed by a series of collimating slits placed in front of and behind the sample. Two-step motors move the arms supporting the source and the detector, and an adjustable sample holder is placed in the optical center of the diffractometer.

The total experimental scattering parameter range, $q = 0.16 - 17.42$ $Å^{-1}$ was obtained recording spectra at given measurement angles θ of 24°, 15.5°, 10.5°, 8.0°, 5.0°, 3.0°, 1.5°, 1.0°, 0.5°, and 0.3°; q can be written as

$$q = 4\pi \sin\theta/\lambda = EC \sin\theta$$

where q is expressed in $Å^{-1}$, λ in Å, and E in keV, and the value of the constant C is 1.014.

The experimental data were then corrected[16−18] normalizing to the incident radiation intensity and dividing by X-ray absorption and polarization coefficients. In addition, the escape peaks were suppressed, and the contributions due to inelastic scattering were subtracted from the observed intensities I (E, Θ).

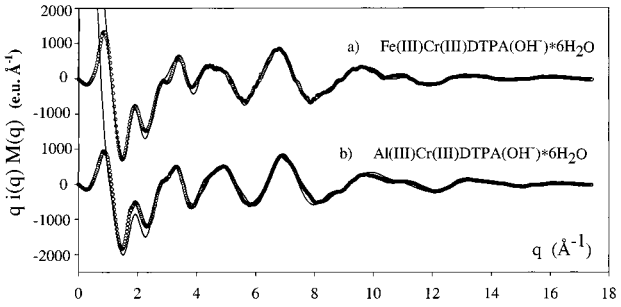

Figure 1. Experimental structure functions in the form $qi(q)M(q)$ (○) and the theoretical curve (—) calculated for two molecules of complexes (a) $Fe(OH)CrDTPA(H_2O)_6$ and (b) $Al(OH)CrDTPA(H_2O)_6$.

Atomic scattering factors, f_h (q), were taken from International Tables.[19] The static structure function

$$i(q) = I_{coh}(E,\Theta) - \sum f^2_h(q)$$

was then calculated. The radial distribution $D(r)$ is

$$D(r) = 4\pi r^2\rho_0 + 2r\pi^{-1}\int_0^{q_{max}} qi(q)M(q)\sin(rq)\,dq$$

where q indicates the scattering parameter, ρ_0 is the average electron density of the sample ($\rho_0 = (\sum_h n_h f_h(0))^2 \cdot V^{-1}$), V is the stoichiometric unit volume chosen, and $M(q)$ is a modification factor defined by

$$f^2_{Cr}(0)/f^2_{Cr}(q)\exp(-0.01q^2)$$

The experimental radial distribution functions are also shown as Diff(r) = $D(r) - 4\pi r^2\rho_0$. Theoretical peaks were calculated performing Fourier transform of the theoretical intensities for the pair interactions

$$i_{ij} = \sum f_i f_j \sin(r_{ij}q)(r_{ij}q)^{-1}\exp(-{}^1/_2\sigma^2_{ij}q^2)$$

The same sharpening function was run for handling both experimental and theoretical data setting the rms variation over the distance as σ_{ij}. The experimental apparatus and technique are described in detail elsewhere.[7−10,14,16,18]

The X-ray data treatment and the kind of information provided by the data have been discussed at length in earlier works cited herein.

3. Results

The experimental structure functions of $Al(OH)CrDTPA(H_2O)_6$ and $Fe(OH)CrDTPA(H_2O)_6$ exhibit the typical behavior of amorphous samples. They are very similar and show a similar oscillation period and amplitude. This suggests that the introduction of the second metal ion does not modify the structure of the primary complex. The functions for the complexes Fe(III) and Al(III) are shown in Figure 1a and b for the range 0−18 $Å^{-1}$.

The experimental radial distribution functions of the samples in the Diff(r) form over the range 0−15 Å reported in Figure 2a and b show two well-defined peaks at about 2.00 and 3.00 Å, one smaller one at around 4.00 Å with a hump at around 4.50 Å, and a large peak centered between 7.00 and 8.5 Å. No

(12) Subramaniam, V.; Lee, K. W.; Hoggard, P. E. *Inorg. Chim. Acta* **1994**, *216*, 155−161.
(13) Crans, D. B.; Jiang, F.; Andreson, O. P.; Miller, S. M. *Inorg. Chem.* **1998**, *37*, 6645−6655.
(14) (a) Caminiti, R.; Sadun, C.; Rossi, V.; Cilloco, F.; Felici, R. XXV Italian Congress on Physical Chemistry, Cagliari, Italy, 1991. (b) Caminiti, R.; Sadun, C.; Rossi, V.; Cilloco, F.; Felici, R. Patent n° RM/93 01261484, June 23, 1993.
(15) Ballirano, P.; Caminiti, R.; Ercolani, C.; Maras, A.; Orrù, A. *J. Am. Chem. Soc.* **1998**, *120*, 12798−12807.
(16) Nishikawa, K.; Iijima, T. *Bull. Chem. Soc. Jpn.* **1984**, *57*, 1750.
(17) Fritsch, G.; Keimel, D. A. *Mater. Sci. Eng.* **1991**, *134A*, 888.
(18) Carbone, M.; Caminiti, R.; Sadun, C. *J. Mater. Chem.* **1996**, *6*, 1709.
(19) *International Tables for X-ray Crystallography*; Kynoch Press: Birmingham, England, 1974; Vol. 4.

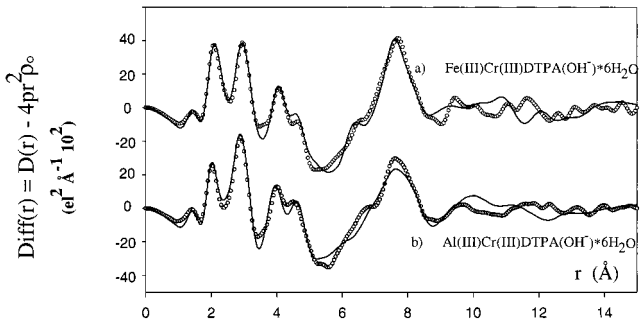

Figure 2. Experimental radial distribution function in the form Diff(r) = $D(r) - 4\pi r^2\rho_\circ$ (○) and the theoretical peak shape function (—) calculated for two molecules of complexes (a) Fe(OH)CrDTPA$(H_2O)_6$ and (b) Al(OH)CrDTPA$(H_2O)_6$.

other peaks were observed. The curves indicate that the samples are unstructured over about 10 Å and then become completely amorphous.

The peaks at 2.00 Å, present in both experimental samples, are due to the interactions of metal ions with the oxygen or nitrogen atoms in the complex molecules.

The height and width of the peaks at 3.00 and especially at 7.50 Å suggest that metal−metal interactions are involved. These interactions can be intramolecular for the first peak and intermolecular for the second peak.

4. Discussion

Numerous structural analyses of complexes formed by DTPA with metals are reported in the current literature. Most of them concern complexes with lanthanides (Ga, Yb, Eu) which have remarkably high coordination numbers and are thus able to coordinate all of the eight DTPA donor atoms, 5 O and 3 N.[20−23] However, the coordination of metals belonging to the transition metals series (Cr,Fe,Ni) has not received as much attention.

Nonetheless, the crystalline structure of FeH_2DPTA and Na_2-(FeDPTA)[24] is well known, the Fe(III) ion being octahedrally or 7-fold coordinated (4 O and 3 N). On the basis of this knowledge, we systematically analyzed our data to determine the samples' structure.

First we analyzed the complex containing Fe(III). The higher electron content of Fe(III) as compared to that of Al(III) makes metal−ligand interaction more readily distinguishable than intraligand interaction.

When iminodiacetate chelators bind the metal ion, several different structures are possible. The first step toward model construction was to determine the possible coordination geometry of the Cr(III) and Fe(III) ions.

We assumed that the small peak, at around 1.50 Å, in the Diff(r) was attributable only to directly bound atoms in the DTPA molecule. The interactions between two successive nondirectly bound atoms appear at distances of over 2.0 Å and are independent of the ligand molecular configuration. Therefore we subtracted the theoretical radial distribution function of the

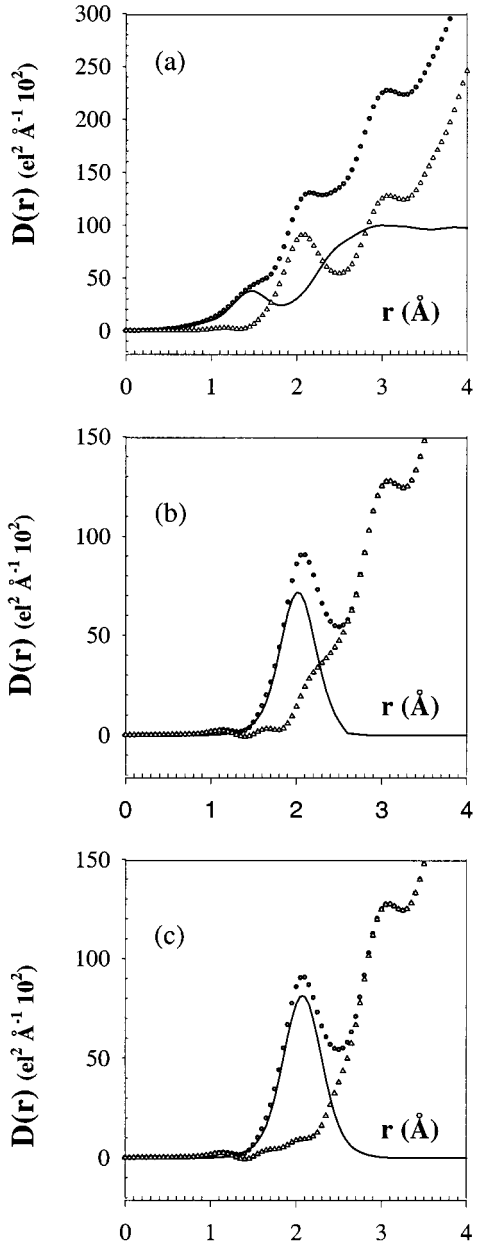

Figure 3. (a) Experimental radial distribution function [$D(r)_{exp}$] of complex Fe(OH)CrDTPA$(H_2O)_6$ [○]; theoretical peak shapes [TPS] function calculated for a possible conformation of DTPA molecule [—]; difference curve = $D(r)_{exp}$ − TPS [△]. (b) Difference curve from Figure 3a (○); theoretical peak shapes calculated for six interactions of Cr−O and four interactions of Fe−O (—); their difference curve [△]. (c) Difference curve from Figure 3a (○); theoretical peak shapes calculated for six interactions of Cr−O and six interactions of Fe−O (—); their difference curve [△].

DTPA molecule structure from the experimental distribution function of the Fe(OH)CrDTPA$(H_2O)_6$ complex. The resulting "difference" curve allows us to determine the number of first neighbor atoms around the metal ions, since in so doing the residual peak at 2.0 Å represents the metal ion−ligand interaction. In Figure 3a the experimental and theoretical radial distribution functions as well as their difference are shown. In this way we can determine coordination numbers, bond distances, and the kind of metal−ligand interaction. Figure 3b and c gives the difference curve calculated as above as well as the theoretical curves for several ion coordination models.

(20) Ruloff, R.; Gelbrich, T.; Hoyer, E.; Sieler, J.; Beyer, L. *Z. Naturforsch.* **1998**, *53B*, 955−959.
(21) Inoue, M. B.; Inoue, M.; Fernando, Q. *Inorg. Chim. Acta* **1995**, *232*, 203−206.
(22) Bronca-Cabarrecq, C.; Fava, O.; Mosset, A. *J. Chem. Crystallogr*. **1999**, *29*, 81−86.
(23) Maupin, C. L.; Mondry, A.; Leifer, L.; Riehel, J. P. *J. Phys. Chem*. A **2001**, *105*, 3071−3076.
(24) Finnen, D. C.; Pinkerton, A. A.; Dunham, W. R.; Sands, R. H.; Funk, M. O., Jr. *Inorg. Chem.* **1991**, *30*, 3960−3964.

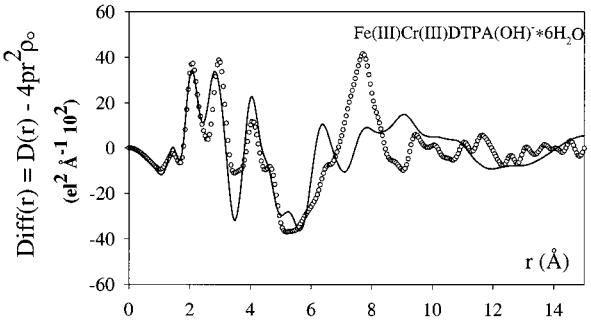

Figure 4. Experimental radial distribution function in the form Diff(r) = $D(r) - 4\pi r^2\rho_\circ$ (○) and the theoretical peak shape function (—) calculated for one molecule of complex Fe(OH)CrDTPA$(H_2O)_6$ involving all of the N atoms in the metal's coordination sphere.

The Cr(III) ion is known to exhibit an octahedral arrangement[25] when hosting electron donor atoms, so we generated a model involving six oxygen atoms. At this point, it was not possible to distinguish whether oxygen atoms alone are involved or if nitrogen atoms are present too, given the small difference in electron content. We calculated the difference between the areas of the peaks in the theoretical distribution functions smaller than 5%. The nature of the atoms belonging to the first coordination sphere can be subsequently determined. The peak for the second neighbor distances of the metal ions is closely dependent upon ligand structure. It is possible to fit it with a ligand molecular conformation, which involves determining the nature of the first sphere donor atoms. Figure 3b and c shows the theoretical curves for the Cr(III) octahedral model, and the two possible coordination structures, tetrahedral and octahedral, of the Fe(III) are shown. Figure 3b refers to the model of the tetrahedral coordinated Fe(III) and to its difference with the experimental distribution function. In the latter curve a well-defined residual peak can be observed at 2.0 Å. Figure 3c refers to the model of the octahedrally coordinated Fe(III). In this case, the difference curve exhibits no residual peak, and we can thus assume that the Fe(III) ion has octahedral arrangement.

Once we had determined the coordination geometry of the metal ions, we examined the optimal distance between the DTPA atoms involved that could be achieved by several molecular conformations.

For the peak at 3.0 Å, several conformational models of the DTPA molecule were tested.

The first tested conformations were derived from those proposed in the literature for solid state and solution chemistry of aminocarboxylate complexes. The aminocarboxylate groups were considered to behave as tridentate groups. The octahedral configuration around the Cr atom was reached by four O atoms and two N atoms; the octahedral configuration around the Fe atom was reached by five O atoms and one N atom. The coordination of the N atom to the Fe ion implies, for the four C atoms belonging to the involved aminocarboxylate group, distances included in the range 2.70−2.80 Å. Therefore the second peak was located at a shorter distance with respect to the experimental one.

In Figure 4 the experimental radial distribution function is reported and compared with the theoretical one obtained from the model shown in Figure 5. This model shows the better agreement between the experimental and the theoretical function,

(25) Sharam, C. L.; Mishra, V. P. *J. Indian Chem. Soc.* **1983**, *60*, 809−812.

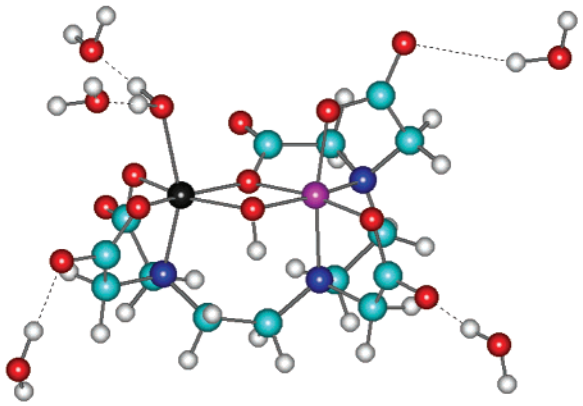

Figure 5. Structural model of complex Fe(OH)CrDTPA$(H_2O)_6$ involving all of the N atoms in the metal's coordination sphere.

Table 1. Distance of the Octahedral Arrangements of Cr(III) and Fe(III)

	atom	r [Å]		atom	r [Å]
Cr(III)	O1	1.99	Fe(III)	O1	1.90
	O6	1.99		O6	1.90
	O2	2.08		O4	2.15
	O3	2.08		O5	2.15
	N1	2.02		W1	2.15
	N2	2.02		W2	2.15
	Fe	3.10			

among all the tested models involving the three N atoms in the coordination spheres of the metal ions.

Good agreement between the experimental radial distribution function and the theoretical peak shape function can only be obtained by assuming a binuclear complex having a Cr−Fe interaction obtained by bridging the metal ions via O atoms. The model that provides the best agreement between experimental and theoretical functions also indicates that the Cr(III) ion coordinates four oxygen atoms and two nitrogen atoms. The distances between Cr(III) and Fe(III) ions and ligands in octahedral arrangement are reported in Table 1.

The water molecules not directly bound as ligand in the metal ion coordination sphere also need to be considered in the complete structure of the complex. Their localization is of prime importance for the peak centered at 4.0−4.5 Å. These molecules might be positioned within the second coordination sphere of the water molecules completing the first Fe(III) coordination sphere. However, only two molecules are involved in the second one, as otherwise the theoretical peak at 4.5 Å would be too high as compared to the experimental one. Figure 6 shows the experimental radial distribution function and the theoretical peak shapes for the ball-and-stick model shown in Figure 7.

The model generated for the Fe(OH)CrDTPA$(H_2O)_6$ yields a structure that excludes long-range interactions. Thus, we can affirm that the peak located at around 7.5 Å in the experimental radial distribution is generated by intermolecular interaction. Careful examination of the experimental radial distributions points reveals how the other molecules should be arranged so as to fit the peak at 7.5 Å.

To facilitate representation of the molecular arrangements, the molecule has been positioned such that the Fe−Cr axis is aligned with the x axis and oriented so that the metal ions and the bridging oxygen atoms lie in the xy plane. When considering two molecules, the Fe(III)−Cr(III) intermolecular interactions

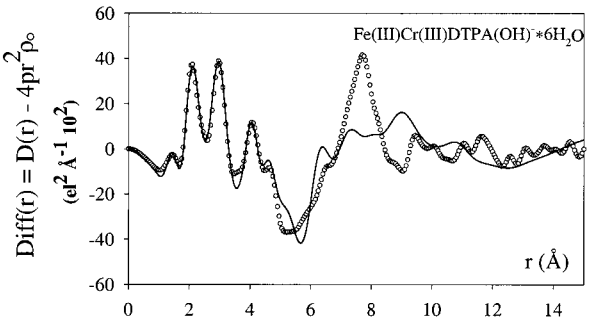

Figure 6. Experimental radial distribution function in the form Diff(r) = $D(r) - 4\pi r^2\rho_\circ$ (○) and the theoretical peak shape function (—) calculated for the better configuration model of one molecule of complex Fe(OH)-CrDTPA$(H_2O)_6$.

Table 2. Root Mean Square (rms) σ_{pq} Values Used in the Model of Fe(OH)CrL$(H_2O)_6$

range (r, Å)	σ_{pq}
$0 < r \leq 1.80$	0.050
$1.80 < r \leq 3.40$	0.115
$3.40 < r \leq 4.85$	0.150
$4.85 < r \leq 8.40$	0.185
$8.40 < r \leq 13.00$	0.230
$r > 13.00$	0.340

are more important than the M−O, M−N, and M−C interactions. One M−M interaction generates a peak, in the theoretical peak shape function, 3 or 4 times broader than that of the other interactions.

To fit the peak at 7.5 Å, we analyzed how two molecules might interact. First the two molecules were aligned, a short distance apart, along the x axis. However, with this configuration, besides the main contribution at 7.5 Å due to a double M−M interaction, two other contributions are observed at 4.5 and 10.5 Å. This would produce two peaks that are not present in the experimental pattern.

Next the molecules were aligned along the y axis. Again this did not produce satisfactory results. By aligning two molecules along the y axis, we obtained two M−M interactions at 7.2 Å and two at 7.8 Å that are compatible with the experimental data. This configuration generates short-range interactions with the result that the first peaks are higher than the experimental curve.

At this point, two molecules were aligned along the z axis. Similarly to the other two arrangements, the second molecule was placed in the same configuration as the first, rotated around the x axis and around the y axis at different angles. All the models generated by these configurations were tested. The best fit for each configuration was obtained by calculating the least squares between the experimental and theoretical data, shifting the second molecule along the three axes.

The best result was obtained by shifting the second molecule, in the same configuration as the first, without rotating it. The Cr(III) atom is positioned at $x = -0.665$, $y = -2.010$, and $z = -7.288$, assuming the Cr(III) atom of the first molecule as a reference for the origin of the Cartesian coordinates. The theoretical structure function and the theoretical peak shape function calculated for the model shown in Figure 8 are compared with the experimental functions in Figure 1a and Figure 2a, respectively.

The same mean square deviation was assigned calculating the theoretical radial distribution for each distance falling within a certain range. Six fixed root-mean-square values (rms σ_{pq}) were used for curve fitting. Thus the number of parameters (σ_{pq}) used for fitting was much smaller than the number of pairs of distances contained in the model. The σ_{pq} are given in Table 2.

The experimental structure function and radial distribution function of the complex containing Al(III) (see Figures 1b and

Table 3. Distance of the Octahedral Arrangements of Cr(III) and Al(III)

	atom	r [Å]		atom	r [Å]
Cr(III)	O1	1.99	Al(III)	O1	1.90
	O6	1.99		O6	1.90
	O2	2.08		O4	1.95
	O3	2.08		O5	1.95
	N1	2.02		W1	1.95
	N2	2.02		W2	1.95
	Al	3.05			

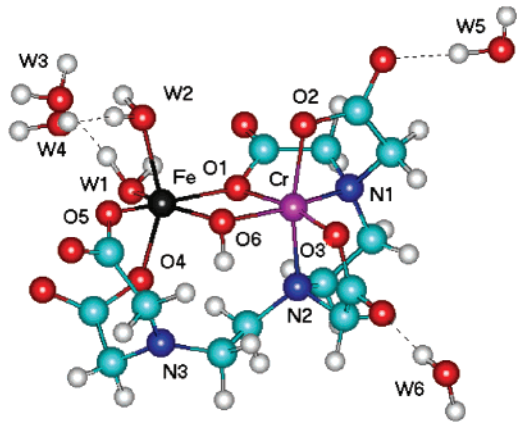

Figure 7. Structural model of the better configuration model of complex Fe(OH)CrDTPA$(H_2O)_6$.

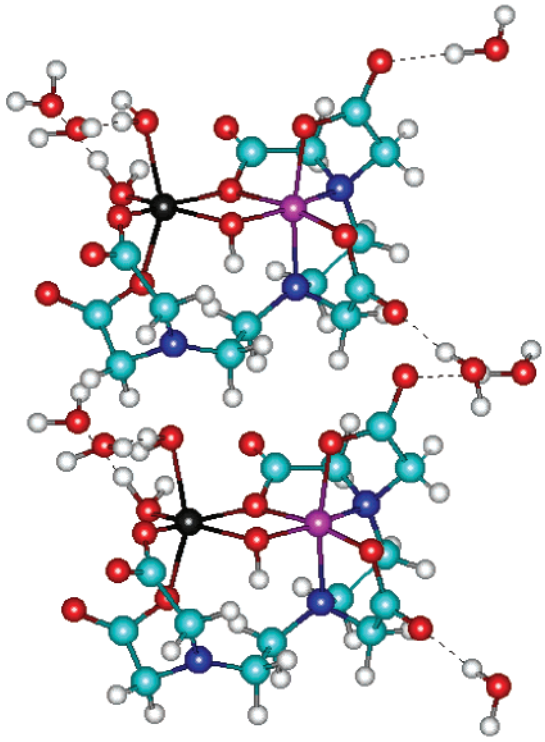

Figure 8. Structural model of the arrangement of two molecules of complex Fe(OH)CrDTPA$(H_2O)_6$.

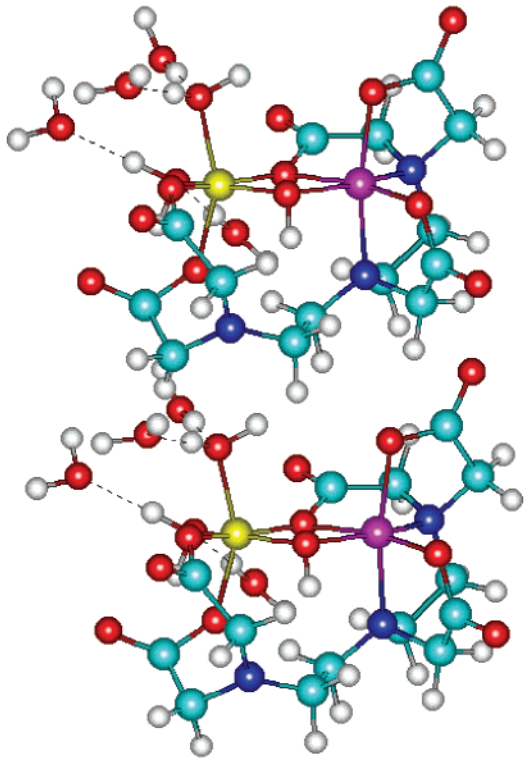

Figure 9. Structural model of the arrangement of two molecules of complex $Al(OH)CrDTPA(H_2O)_6$.

2b, respectively) are very similar to those of the complex containing Fe(III). These functions exhibit similar oscillation periods and amplitudes; thus we assumed that the structure found for the first complex could also fit the experimental data of the second.

Thus the structure of the complex Cr(III)DTPA, determined for the Fe(III) complex, was maintained. Only the coordination distances of the Al(III) ion were changed. Two water molecules provide two oxygen atoms. The distances of the bridging oxygen atoms are kept unchanged; the minor difference between the Fe(III)−Cr(III) and Al(III)−Cr(III) distances is determined by a small change in the angle OAlO. The configuration of the DTPA molecule should not change significantly as the carboxylic oxygen atoms binding the Al(III) atom approach. The distances for Cr(III) and Al(III) ions in the octahedral arrangement are given in Table 3. The only significant difference between the two complexes lies in the position of the water molecules. In $Al(OH)CrDTPA(H_2O)_6$ the two water molecules coordinated to the Al(III) atoms each have two water molecules in the second coordination sphere. The water molecules representing the second coordination sphere are required in this case to fit the peak at 4.5 Å, which is higher than that of the Fe(III) complex.

Table 4. Root Mean Square (rms) σ_{pq} Values Used in the Model of $Al(OH)CrL(H_2O)_6$

range (r, Å)	σ_{pq}
$0 < r \leq 2.40$	0.060
$2.40 < r \leq 3.40$	0.090
$3.40 < r \leq 4.85$	0.150
$4.85 < r \leq 8.40$	0.260
$8.40 < r \leq 13.00$	0.300
$r > 13.00$	0.400

The position of the second molecule was fitted as for $Fe(OH)CrDTPA(H_2O)_6$. The Cr(III) atom of the second molecule was positioned at $x = -0.309$, $y = -1.634$, and $z = -7.373$ when the Cr(III) atom of the first molecule was located at the origin of Cartesian coordinates. The theoretical structure function and the theoretical peak shape function, calculated using this model and shown in Figure 9, are compared with the experimental functions in Figures 1b and 2b, respectively. The values of σ_{pq} and the relative distance range are given in Table 4.

5. Conclusions

On the basis of the results obtained, the following considerations can be drawn: X-ray analysis is especially suitable for providing information as to how the metal ions interact with their surroundings. Thus, all the atoms constituting the molecule can be localized, even for an amorphous sample. The complexes studied here show peculiar aspects. They are binuclear with the two metal ions bridging via oxygen atoms.

Two molecules interact in a strong manner, with a defined position, as shown by the large peak centered at 7.0 Å. There is no evidence of further preferential interaction between molecules that are further apart. In fact, well-defined peaks are not observed in the experimental distribution function after 8.0 Å. When one molecule is considered as a reference, only its nearest neighbor has a defined position; the others have highly random spatial distribution as compared to that of the first molecule and are not arranged in any particular structure.

Acknowledgment. The authors of this paper are indebted to Professor Ruggero Caminiti at the "La Sapienza" University in Rome for his helpful and stimulating comments and discussion.

JA010676+